Carrier-injection-based electro-optic modulator on silicon-on-insulator with a heterogeneously integrated III-V microdisk cavity

Liu Liu,[1,*] Joris Van Campenhout,[2] Günther Roelkens,[1] Richard A. Soref,[3] Dries Van Thourhout,[1] Pedro Rojo-Romeo,[4] Philippe Regreny,[4] Christian Seassal,[4] Jean-Marc Fédéli,[5] and Roel Baets[1]

[1]*INTEC Department, Photonics Research Group, Ghent University-IMEC, St-Pietersnieuwstraat 41, 9000 Ghent, Belgium*

[2]*Current address: T. J. Watson Research Center, IBM, 1101 Kitchawan Road, Yorktown Heights, New York 10598, USA*

[3]*Sensors Directorate, Air Force Research Laboratory, Hanscom Air Force Base, Massachusetts 01731, USA*

[4]*Institut des Nanotechnologies de Lyon INL-UMR5270, CNRS, Université de Lyon, Ecole Centrale de Lyon, Ecully F-69134, France*

[5]*CEA-LETI, Minatec 17 rue des Martyrs, 308054 Grenoble, France*

**Corresponding author: liu.liu@intec.ugent.be*

Received September 5, 2008; revised September 30, 2008; accepted October 1, 2008; posted October 3, 2008 (Doc. ID 101210); published October 28, 2008

A compact electro-optic modulator on silicon-on-insulator is presented. The structure consists of a III-V microdisk cavity heterogeneously integrated on a silicon-on-insulator wire waveguide. By modulating the loss of the active layer included in the cavity through carrier injection, the power of the transmitted light at the resonant wavelength is modulated; ~10 dB extinction ratio and 2.73 Gbps dynamic operation are demonstrated without using any special driving techniques. © 2008 Optical Society of America

OCIS codes: 130.0250, 130.4110.

Electro-optic modulators on silicon-on-insulator (SOI) are critical components for future optical interconnections [1–7]. The refractive index of silicon can be modified through carrier injection or depletion [8]. This effect, so-called the free carrier dispersion (FCD), is to our knowledge so far the best all-silicon solution to achieve a fast and efficient optical modulator on SOI owing to the fact that silicon exhibits very weak or even zero coefficients of other common electro-optic effects, e.g., the Pockels effect, the Kerr effect, and the Franz–Keldysh effect. Devices based on carrier depletion can offer a fast operation speed (e.g., 40 Gbps in [1]). However, owing to the small light confinement in the depleted region, the interaction length of the device has to be large [1], or a high drive voltage is required [2], to ensure enough modulation depth. On the other hand, the carrier injection approach can improve the modulation efficiency, but the speed is limited by the slow carrier injection/recombination processes in silicon [3–6]. Based on carrier injection, <1 Gbps nonreturn-to-zero (NRZ) modulation has been reported originally [3,4], and ~10 Gbps has been achieved by using the preemphasis driving technique [5,6].

III-V compound semiconductors can provide a variety of electro-optic effects for light modulation, and they are often much faster and stronger than those in silicon. Heterogeneous integration of the III-V active material with the silicon passive waveguide would be a promising approach to improve the performance of such a modulator on SOI. Recently, a hybrid silicon evanescent modulator has been demonstrated employing the electro-absorption effect in a III-V layer bonded on top of an SOI waveguide [7]; 10 Gbps operation speed and 10 dB extinction ratio has been achieved with a device length of several hundred micrometers. In this Letter, we introduce a carrier-injection-based microdisk modulator on the heterogeneous III-V/SOI platform. By using a resonant structure, the dimension of such a modulator is shrunk below 10 μm. The working principle here is based on the fact that the loss–gain of the active material in the microdisk cavity (MDC) varies with current injection; ~10 dB extinction ratio and 2.73 Gbps operation speed are achieved in the proposed device without using any special driving techniques.

Figure 1 shows a sketch of the experimental setup. The cavity was formed by a III-V microdisk with a diameter of 7.5 μm and a thickness of 1 μm. This III-V layer was bonded on top of an SOI wire waveguide (dimension: 500 nm × 220 nm) prior to the definition of the disk. A p-i-n diode with three strained InAsP quantum wells (absorption edge at ~1620 nm) was embedded in this III-V layer along the vertical direction for carrier injection. The structure is actually the same as what has been used for a microdisk laser in [9], where a detailed description and parameters can be found. TE-polarized light from a tunable laser was coupled into the SOI waveguide. The input light then interacted with the whispering-gallery mode (WGM) circulating around the perimeter of the MDC through vertical evanescent coupling. The WGM experiences either a loss or a gain depending on the bias current.

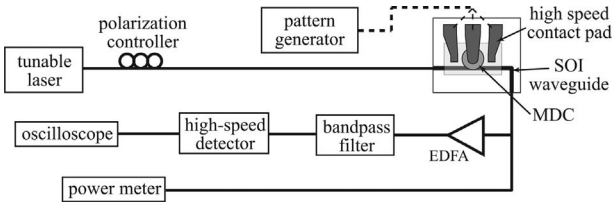

Fig. 1. Sketch of the experimental setup.

The transmitted light in the SOI waveguide was collected. For dynamic measurements, it was first amplified by an erbium-doped fiber amplifier (EDFA), and a bandpass filter was employed to suppress the spontaneous emission noise.

The transmission spectra with different bias currents/voltages under static operations are shown in Fig. 2. A time-domain coupled-mode theory is used to analyze the interaction of the fundamental WGM mode with the SOI waveguide mode [10]. The relation between the transmission T and the frequency ω of the input laser is expressed as

$$T = T_0 \left| 1 - \frac{\alpha_c v_g}{j(\omega - \omega_0) + \frac{\alpha_c v_g}{2} + \frac{\alpha_a v_g}{2} + \frac{\alpha_o v_g}{2}} \right|^2, \quad (1)$$

where ω_0 is the resonant frequency of the WGM, v_g is the group velocity, α denotes various losses of the WGM per unit length, and α_c is the distributed coupling loss to the SOI waveguide; α_a is the loss (being minus the gain) of the active layer (i.e., the quantum wells), and it is a monotonically decreasing function of the bias current; α_o includes other internal losses; $T_0 \approx 0.5$ denotes the extra insertion loss due to the coupling to higher-order modes supported by the 1-μm-thick III-V layer [9]. It is obvious that the transmission $T = T_0$ when the frequency ω of the input laser is far away from the resonant frequency ω_0. At resonance, i.e., $\omega = \omega_0$, the transmission drops, and the extinction ratio is related to the amount of the various losses. When no current is injected, α_a is large as compared to other losses due to the high band-to-band absorption of the active layer. From Eq. (1), we can find that the transmission is still close to T_0 even at resonance. As also shown in Fig. 2, no dip in the transmission spectrum is observed for zero bias. When the injection current increases, α_a decreases accordingly. The transmission dip also becomes more and more obvious. Particularly, when $\alpha_a + \alpha_o = \alpha_c$ (the critical-coupling condition [10]), the transmission will decrease to zero at the resonant frequency. The highest extinction ratio of ~16 dB was obtained at 540 μA/1.18 V. It is worthwhile to note that the positions of the transmission dips also vary under different bias conditions. This dip first blueshifts as the current increases owing to the increase of the carrier density similar to the FCD effect employed in the all-silicon modulators [1–6]. As the bias increases further, the thermo-optic effect starts to take over, and a redshift is therefore observed.

In the above analysis, we ignored the impact of the input laser power. Indeed, the stimulated excitation or recombination of the carriers caused by the resonant photons in the MDC would affect the value of α_a and the transmitted power. To study this effect, we recorded the extinction ratios at different input power levels, and the results are shown in Fig. 3. For a 540 μA bias the extinction ratio drops obviously as the input power increases, and it is saturated around 10 dB, while for a 400 μA bias the extinction ratio is rather stable within 10 dB ±1 dB at different power levels. This can be explained if the active layer is at transparency (i.e., $\alpha_a = 0$) at a 400 μA bias. In this case, no stimulated excitation or recombination occurs. Thus, α_a and the extinction ratio is not affected by the input power, while at a higher bias the active layer exhibits a gain (i.e., $\alpha_a < 0$). The stimulated recombination of the carriers gradually saturates this gain owing to the increased photon density in the MDC and α_a increases back to 0 at a high laser power. As a result, the extinction ratio drops to the value at transparency, i.e., ~10 dB. Similar behavior was also observed at a lower bias, where the extinction ratio increases as the input power increases owing to the absorption bleaching of the active layer. For a practical modulator, the modulation depth should not depend on the input laser power. Therefore, we can conclude that the best operation point for the proposed device should be at the bias of 400 μA/1.1 V. This current level is still high as compared to that in the all-silicon modulators based on FCD [3–5], partially owing to the disk structure used here. The current going through the center part of the disk is actually wasted. It can be reduced by creating a central hole or employing an ultrasmall disk [11]. Besides through carrier injection as proposed here, the loss of a III-V active layer can also be modified via a fast field effect, e.g., the electro-absorption effect under a reverse bias [7]. This can largely reduce the power consumption.

The dynamic result of the optical modulation is shown in Fig. 4, where the MDC was driven with an electric signal from a pattern generator. The electric driving signal was a square wave from 0 to 1.1 V at a frequency of 340 MHz with a rise–fall time of ~30 ps. The output laser was weak and noisy due to the high butt-coupling loss to the SOI waveguide, and for a

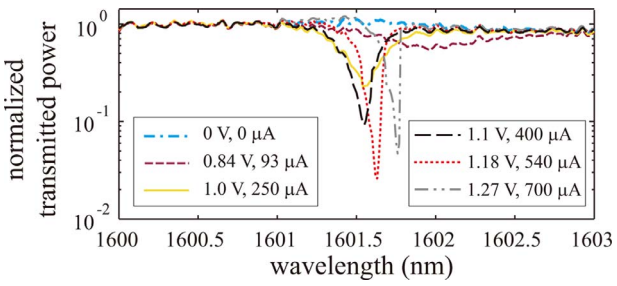

Fig. 2. (Color online) Static transmission spectra through the MDC with different bias voltages and currents. The lasing threshold current of the MDC is 800 μA.

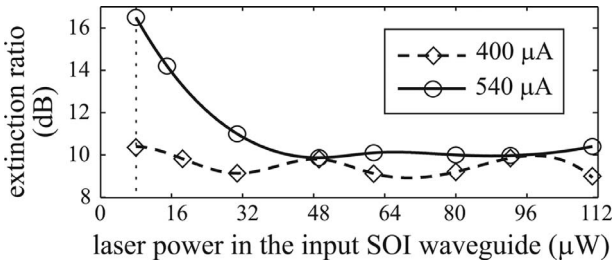

Fig. 3. Measured extinction ratio as a function of the laser power in the input SOI waveguide. Parameters are the bias currents. The dotted curve denotes the power level used in Fig. 2.

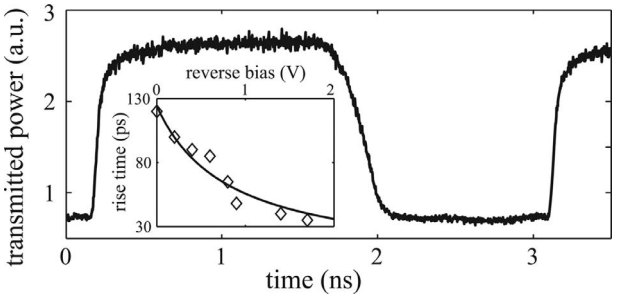

Fig. 4. Optical response of the modulator under a square wave signal with a voltage level of 0–1.1 V and a frequency of 340 MHz. The inset shows the rise time as a function of the reverse bias voltage.

clear demonstration the averaged waveform is actually shown here. The optical modulation depth is ~6 dB, slightly less than the static result, due to the significant spontaneous emission from the EDFA. The dependence of the modulation depth on the input laser power in the dynamic case was also tested. No obvious fluctuation was observed. This confirms the results in Fig. 3. The rise and the fall times of the modulated light is 120 and 350 ps, respectively, which includes the response time of the electric driving signal. The difference in the rise and the fall times results from the resonant wavelength shift at different biases as discussed above. This means that both the gain–loss and the resonant wavelength modulation exists in the present device. Further investigation suggests that the resonant wavelength shift is actually the dominant effect here. Employing a reverse bias can increase the carrier extraction speed and decrease the rise time as shown in the inset of Fig. 4. A 35 ps rise time was obtained with −1.8 V of bias. Nonetheless, the speed of the proposed device is still limited by the much slower fall time, i.e., the carrier injection speed. In Fig. 5, we show the waveform of the electric driving signal and the corresponding optical signal using a 32-bit NRZ pattern at a bit rate of 2.73 Gbps. One can see that the information was transferred onto the laser beam in an inverted way. Note that we obtained this operation speed without using any special driving techniques, while for the all-silicon carrier-injection-based devices 0.4 Gbps NRZ modulation was originally reported in this case [3]. Although the speed of those devices has been pushed to >10 Gbps with the preemphasis technique [5,6], this approach can also be employed to improve the carrier injection speed in the present device and increase the overall operation speed.

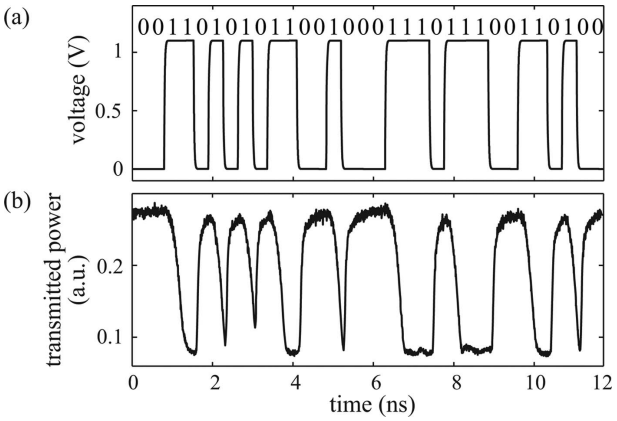

Fig. 5. Waveform of a 32-bit NRZ signal at 2.73 Gbps applied on (a) proposed modulator and (b) corresponding optical signal.

In conclusion, we have introduced an electro-optic modulator with a III-V MDC heterogeneously integrated on an SOI wire waveguide. By modulating the bias current, the active layer in the MDC works between a high loss and transparency. Therefore, the drop efficiency of the cavity, as well as the power of the transmitted light, is also modulated; ~10 dB extinction ratio and 2.73 Gbps dynamic operation have been demonstrated without using any special driving techniques.

L. Liu acknowledges Interuniversity Attraction Poles for a postdoctoral grant. G. Roelkens acknowledges Fund for Scientific Research–Flanders for a postdoctoral grant. This work is supported partially by the European Union (EU)-funded projects Photonic Interconnect Layer on CMOS by Wafer-Scale Integration and Wavelength Division Multiplexed Photonic Layer on CMOS.

References

1. A. Liu, L. Liao, D. Rubin, J. Basak, Y. Chetrit, H. Nguyen, R. Cohen, N. Izhaky, and M. Paniccia, Electron. Lett. **23**, 1196 (2007).
2. M. R. Watts, D. C. Trotter, R. W. Young, and A. L. Lentine, in *5th IEEE International Conference on Group IV Photonics* (IEEE, 2008), paper WA2.
3. Q. Xu, B. Schmidt, S. Pradhan, and M. Lipson, Nature **435**, 325 (2005).
4. L. Zhou and A. W. Poon, Opt. Express **14**, 6851 (2006).
5. Q. Xu, B. Schmidt, J. Shakya, and M. Lipson, Opt. Express **15**, 430 (2007).
6. W. M. J. Green, M. J. Rooks, L. Sekaric, and Y. A. Vlasov, Opt. Express **15**, 17106 (2007).
7. Y. Kuo, H. Chen, and J. E. Bowers, Opt. Express **16**, 9936 (2008).
8. R. A. Soref and B. R. Bennett, IEEE J. Quantum Electron. **23**, 123 (1987).
9. J. Van Campenhout, L. Liu, P. Rojo-Romeo, D. Van Thourhout, C. Seassal, P. Regreny, L. Di Cioccio, J.-M. Fedeli, and R. Baets, IEEE Photon. Technol. Lett. **20**, 1345 (2008).
10. C. Manolatou, M. J. Khan, S. Fan, P. R. Villeneuve, H. A. Haus, and J. D. Joannopoulos, IEEE J. Quantum Electron. **35**, 1322 (1999).
11. M. Fujita, A. Sakai, and T. Baba, IEEE J. Sel. Top. Quantum Electron. **5**, 673 (1999).